© Photos: DOI: 10.2516/ogst/2013139, IFPEN, X

Dossier

This paper is a part of the hereunder thematic dossier published in OGST Journal, Vol. 69, No. 1, pp. 3-188 and available online here

Cet article fait partie du dossier thématique ci-dessous publié dans la revue OGST, Vol. 69, n°1, pp. 3-188 et téléchargeable ici

DOSSIER Edited by/Sous la direction de : **C. Angelberger**

IFP Energies nouvelles International Conference / Les Rencontres Scientifiques d'IFP Energies nouvelles

LES4ICE 2012 - Large Eddy Simulation for Internal Combustion Engine Flows

LES4ICE 2012 - La simulation aux grandes échelles pour les écoulements dans les moteurs à combustion interne

Oil & Gas Science and Technology – Rev. IFP Energies nouvelles, Vol. 69 (2014), No. 1, pp. 3-188

Oil & Gas Science and Technology – Rev. IFP Energies nouvelles, Vol. 69 (2014), No. 1, pp. 29-40

DOI: 10.2516/ogst/2013122

IFP Energies nouvelles International Conference
Rencontres Scientifiques d'IFP Energies nouvelles

LES4ICE 2012 - Large Eddy Simulation for Internal Combustion Engine Flows
LES4ICE 2012 - La simulation aux grandes échelles pour les écoulements dans les moteurs à combustion interne

LES of Gas Exchange in IC Engines

V. Mittal[1]*, S. Kang[2]*, E. Doran[3], D. Cook[3] and H. Pitsch[4]

[1] *Dept of Mechanical Engineering, Stanford University, CA 94089 - USA*
[2] *Dept of Mechanical Engineering, Sogang University - Korea*
[3] *Robert Bosch Research and Technology Center, Palo Alto - USA*
[4] *Institute for Combustion Technology, RWTH University, Templergraben, Aachen - Germany*
e-mail: mittal1@stanford.edu - skang@sogang.ac.kr - eric.doran@us.bosch.com - David.Cook2@us.bosch.com - h.pitsch@itv.rwth-aachen.de

* Corresponding authors

Résumé — **LES échanges gazeux pour moteurs à combustion interne** — Du fait de la complexité croissante des technologies moteurs et de l'augmentation des points de fonctionnement, il est devenu important de bien comprendre les phénomènes transitoires afin de garantir un fonctionnement stable. Contrairement à la modélisation dite *Reynolds Averaged Navier-Stokes* (RANS) qui ne fournit qu'une information moyennée sur un cycle, la modélisation dite *Large Eddy Simulation* (LES) est capable de simuler les variations cycle à cycle. Ce travail s'appuie ainsi sur une méthodologie LES pour moteur à combustion interne, développée dans une approche de type différences finies. L'approche structurée des algorithmes permet un processus de génération de maillages efficace et pose un cadre favorable pour des méthodes numériques d'ordre supérieure. Une décomposition en blocs paralléles qui est efficace et adaptable résout la difficulté associée au faible rapport d'éléments fluides sur le nombre total d'éléments. Les mouvements des valves et du piston sont gérés respectivement par une approche de découpage de cellules et par la méthode *Arbitrary Lagrangian Eulerian* (ALE). Les conditions dans les collecteurs sont prescrites en utilisant une méthode *Navier-Stokes Characteristic Boundary Conditions* (NSCBC) modifiée. La précision de ce solveur est validée sur des configurations canoniques. Des simulations de flow bench sur une configuration axisymétrique et dans un véritable moteur sont effectuées avec l'approche LES. De plus, les échanges gazeux en condition moteur sont simulés. Dans l'ensemble, l'accord obtenu entre simulations et expériences est bon. Aussi ce cadre peut-il être utilisé pour des calculs moteur, et en particulier des simulations d'écoulements réactifs en LES seront conduites à l'avenir.

Abstract* — *LES of Gas Exchange in IC Engines — *As engine technologies become increasingly complex and engines are driven to new operating points, understanding transient phenomena is important to ensure reliable engine operation. Unlike Reynolds Averaged Navier-Stokes (RANS) studies that only provide cycle-averaged information, Large Eddy Simulation (LES) studies are capable of simulating cycle-to-cycle dynamics. In this work, a finite difference based structured methodology for LES of IC engines is presented. This structured approach allows for an efficient mesh generation process and provides potential for higher order numerical accuracy. An efficient parallel scalable block decomposition is done to overcome the challenges associated with the low ratio of fluid elements to overall mesh elements. The motion of the valves and piston is handled using a dynamic cell blanking approach and the Arbitrary Lagrangian Eulerian (ALE) method, respectively. Modified three-dimensional Navier-Stokes Characteristic Boundary Conditions (NSCBC)*

are used in the simulation to prescribe conditions in the manifolds. The accuracy of the simulation framework is validated using various canonical configurations. Flow bench simulations of an axisymmetric configuration and an actual engine geometry are done with the LES methodology. Simulations of the gas exchange in an engine under motored conditions are also performed. Overall, good agreement is obtained with experiments for all the cases. Therefore, this framework can be used for LES of engine simulations. In the future, reactive LES simulations will be performed using this framework.

INTRODUCTION

With the ever-rising need for better fuel efficiency and lower emissions, development of improved engine technologies is critical. As these technologies become increasingly complex and engines are driven to new operating points, transient phenomenon can become important. When studying strategies such as ultra lean combustion, understanding cycle-to-cycle variability is important, and this is difficult to analyze experimentally due to the inability to ensure repeatable initial conditions. Simulations have the potential to provide insight into the sources of these cyclic variations. However, the Reynolds Averaged Navier-Stokes (RANS) approach that has been used extensively for engine simulations, cannot be used to study such transient behavior because it provides ensemble averaged information. A different methodology that provides cycle resolved information is the Large Eddy Simulation (LES) approach. The advantage of LES lies in the direct computation of the large scale flow structures that enables a better description of the turbulence and ultimately its interaction with chemistry. These improvements facilitate the use of LES for robust design since the effect of small design changes can be captured using LES [1]. However, the computational cost of LES studies is significantly larger than RANS studies. Only very recently have LES studies been conducted to investigate cyclic variations in engines [2-5].

A fundamental requirement for an accurate LES simulation is a stable numerical scheme with minimal dissipation. If a structured framework is used, higher order finite difference schemes with discrete mass, momentum and energy conservation can be used [6]. Use of these schemes ensures that the turbulent energy is not artificially dissipated and small flow structures are retained, leading to a more accurate description of turbulent mixing. Higher order compact filters have also been developed for this framework, which provide a better estimate of the subfilter quantities using a dynamic procedure. A structured framework also allows for easier and faster mesh generation. This helps to reduce the overall time required for a simulation study. Furthermore, a structured domain ensures efficient parallel communication which is essential for scalability to a large number of processors.

Despite these advantages, the structured framework has not been extensively used for LES of engines due to various challenges. First, a large proportion of solid cells are present if a typical engine configuration with cylinder and manifolds, is represented using this framework, leading to dramatically lower code efficiency and improper load balancing. Second, the two-dimensional motion of the valves cannot be represented by structured mesh motion because that will lead to skewed meshes. Finally, resolving small flow passages and complex geometric features with a single structured mesh can lead to large mesh sizes.

In this work, a finite difference based methodology for LES of IC engines is presented that attempts to resolve some of the above issues and provides a robust framework for further development. First, the overall simulation framework is described. Next, certain key elements of the framework including the object motion and the boundary condition description are presented. Finally, various validation cases of the framework are presented including flow bench simulations and gas exchange simulations.

1 SIMULATION FRAMEWORK

1.1 Governing Equations

The Navier-Stokes equations used to describe fluid flow are:

$$\frac{\partial}{\partial t}(\rho) + \frac{\partial}{\partial x_j}(\rho u_j) = 0 \tag{1}$$

$$\frac{\partial}{\partial t}(\rho u_i) + \frac{\partial}{\partial x_j}(\rho u_j u_i) = -\frac{\partial P}{\partial x_i} + \frac{\partial \tau_{ij}}{\partial x_j} \tag{2}$$

where ρ is the density, t is the time, u_j is the velocity in direction j, P is the pressure, and τ_{ij} is the viscous stress tensor. Body forces have been neglected in the above equation. While the above equations can be simplified for low Mach number flows, the Mach number in engine

configurations can be high when the valves first open. Therefore, a compressible formulation is required, and in addition to the above equations, an internal energy equation is solved according to:

$$\frac{\partial(\rho e)}{\partial t}+\frac{\partial\left(\rho u_j e\right)}{\partial x_j}+P\frac{\partial u_j}{\partial x_j}=\tau_{ij}\frac{\partial u_i}{\partial x_j}+\frac{\partial}{\partial x_j}\left(\lambda\frac{\partial T}{\partial x_j}\right)-\frac{\partial q_{\mathrm{FLUX}}}{\partial x_j}-\dot{q}_{\Delta h} \tag{3}$$

where λ is the thermal conductivity, T is the temperature, q_{FLUX} is the enthalpy flux and $\dot{q}_{\Delta h}$ includes heat losses. In the LES framework, a low-pass filter is applied to the above equations to retain information at length scales larger than the filter, while removing higher frequency information. The filter size is prescribed as the local grid size in this work. The subgrid scale effect is modeled using the dynamic Smagorinsky model [7]. A weighted averaging is performed backward in time over Lagrangian trajectories of fluid particles [8]. Similar dynamic models are used for modeling the subgrid effect on scalars [9].

1.2 Numerical Framework

A high-order accurate finite difference code is used as the backbone for the simulations performed in this work. The numerical schemes used for discretizing the equations are based on the work in [10], where a staggered representation of the flow quantities is used. Kinetic energy is conserved discretely, allowing accurate simulation of turbulent reacting flows. In an engine, the convective CFL (Courant-Friedrichs-Lewy) can be much lower than the acoustic CFL. Therefore, using implicit time advancement methods can provide good speedup by allowing a much larger time step. However, it is found that the speedup is negated by the increased computational time of the method. Therefore, an explicit 2nd order, 5-stage explicit Runge-Kutta (RK) scheme [11] is used in this work. While the theoretical CFL limit of this RK scheme is 3.52, a lower CFL below 2 is used since viscous terms are present.

Even with high order methods, some filtering is required to remove the high frequency wave numbers that cannot be resolved on the grid. However, it is important to ensure that filtering only removes the high frequency information and does not affect the turbulent structures globally. This is accomplished through the use of a sixth order accurate implicit filtering procedure described in [12]. The constant prescribing the quality of the filtering, α, is set as 0.25 here. At points near the wall, the order of the filter is reduced locally depending on the available number of neighboring points.

The engine geometry is represented with a structured Cartesian geometry in this work. The mesh is stretched locally to obtain higher resolution near geometric objects such as the valves and piston. In a structured environment, various methods such as the immersed boundary method [13] can be used to represent complex objects on cartesian grids. However, robustness of the conservation properties of the method can become an issue. Another approach is to use overset methods to represent the region near a complex object with a refined grid. The information from this refined grid can be coupled to the solution on the coarser background mesh. However, in this study, a simple stair step representation of the object is used first to assess the quality of the flow solution.

1.2.1 Reduced Cartesian Communicator

In a parallel framework based on SIMD (single instruction, multiple data) such as domain partitioning with the Message Passing Interface (MPI) library, a large ratio of solid cells can lead to severe load imbalance among the processors, resulting in overall reduced computational efficiency. In this work, a different approach is presented which utilizes a Reduced Cartesian Communicator (RCC) to significantly improve the computational efficiency while preserving the benefits of a structured framework.

In this method, the processors span predominantly over the fluid regions of interest. This is accomplished by first creating different structured partition maps of the domain with larger number of regions than the physical number of processors. Next, regions with only solid cells are ignored, and the number of remaining regions is counted. If this number is equal to the number of physical processors, a RCC is setup between these predominantly fluid regions. The solid regions are denoted as empty blocks in this setup.

This method is illustrated using a sample domain shown in Figure 1, where the fluid region is denoted as white, and the solid region is denoted as gray. Figure 1a illustrates a simple structured decomposition of the domain with four processors. As shown, a large number of cells in processors 2-4 are solid regions. Also, the number of cells on every processor is $N/4$, where N is the total number of cells. The decomposition with RCC is shown in Figure 1b with domain partitioning into six regions. Using this decomposition, the fluid region can be represented exactly with four processors, and no solid regions need to be evaluated. The resulting number of cells per processor is $N/6$, which is faster than the simple partitioning method.

While the efficiency improvement by using this method depends on the geometry, it is typically larger for higher number of processors. This occurs because partitioning into more regions leads to smaller partition blocks. Therefore, more complete solid regions can be ignored leading to a reduction in the overall number of solid cells solved. This is highlighted using the geometry shown in Figure 2. The inverse of the number of cells solved per processor can be considered as a measure of efficiency if communication costs are ignored. This value normalized by the total number of cells is shown in Figure 2b for both methods, where $N_{g,x}$ is the number of cells solved per processor, and $N_{g,1}$ is the total number of cells. For a simple structured partition, the ideal speedup is linear with unity slope for increasing number of processors. The speedup of the method presented here is higher due to the reason mentioned above, and the slope of efficiency increase is close to 2. Although this value is true only for the ideal speedup and does not account for increased communication costs, this example illustrates the increased efficiency when this method is used for complex geometry representation.

The method based on RCC presented here is implemented in this work for performing the various simulations used for overall flow validation. The optimal partition is generated using a brute force search of all available partitions for a given number of physical processors. The RCC methodology is also implemented using the existing MPI framework. No additional modification is required to the flow solver.

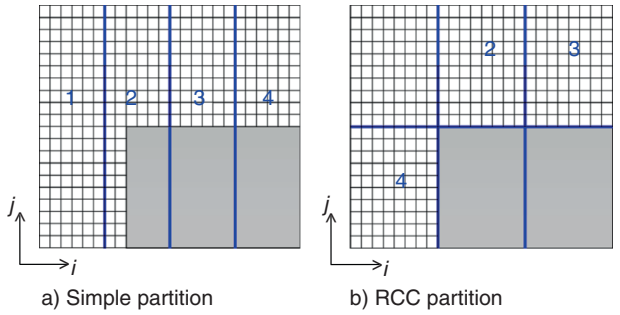

Figure 1

Comparison of RCC partitioning to a simple partitioning in a two-dimensional case. The blue line denotes processor boundaries, and gray color denotes a solid region. The number is the sequential processor ID.

1.3 Navier Stokes Characteristic Boundary Conditions

Prescribing consistent boundary conditions in the manifold is important for accurate engine simulations. Typically, the only information available in the manifold is a pressure which is either measured from experiments or determined from one-dimensional gas dynamics models. While the flow typically comes into the cylinder through

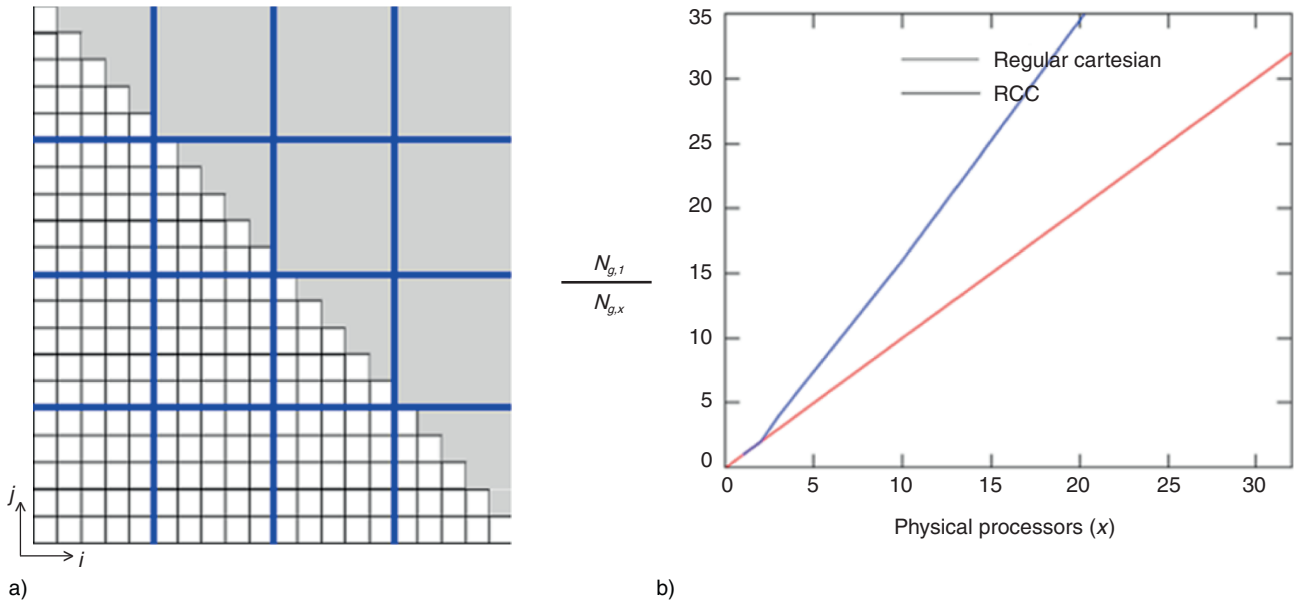

Figure 2

Profiles of the ideal speedup using the regular and RCC partition maps. a) Geometry and sample processor boundaries; b) Comparison of ideal speedup.

the intake manifold, flow can also move upstream in the manifold if the pressure is high in the cylinder when the intake valve is opened. For compressible flows, the Navier Stokes Characteristic Boundary Conditions (NSCBC) [14] are a popular way for prescribing the boundary conditions. The canonical formulation was extended to a three dimensional formulation with transverse terms for better accuracy [15]. However, the formulation is different depending on whether the boundary is an inlet or outlet. The inlet velocity needs to be prescribed at an inlet boundary plane. However, the velocity is not known in the manifold. On the other hand, if the canonical outlet condition is used, the pressure can be prescribed but the bulk flow should be going out of the domain. Therefore, neither of the formulations can be used directly.

In this work, the outlet formulation is modified to allow a consistent boundary condition, the details of which can be found in [15]. The outgoing and incoming acoustic waves in the formulation are calculated using the normal procedure. The entropy wave is described using the standard formula for the outgoing entropy wave if the flow is going out of the domain. However if the flow comes in through the manifold, the entropy wave description is modified to a form typically used for an inlet condition with a target temperature value. The two definitions of the entropy wave are

$$\mathrm{L}_{2,\mathrm{OUT}} = u_i\left(c^2\frac{\partial\rho}{\partial x_i} - \frac{\partial P}{\partial x_i}\right) \tag{4}$$

$$\mathrm{L}_{2,\mathrm{IN}} = -\eta\frac{\rho c R}{L_i}(T - T_0) + \left(c^2\mathscr{T}_1 - \mathscr{T}_5\right) \tag{5}$$

where L_2 is the entropy wave, c is the average speed of sound over the boundary, T is the local temperature, T_0 is the target temperature, η is a relaxation parameter, L_i is a representative length scale in the i direction, and $\mathscr{T}_1$ and $\mathscr{T}_5$ are the transverse terms. This formulation can be used as a consistent boundary condition at the manifold.

Another complexity introduced due to the slanted intake manifold pipes is that the flow is not orthogonal to the boundary. This occurs because considering orthogonal boundaries to the flow leads to stair-step cells at the boundary, leading to additional errors. Instead, a non orthogonal boundary to the flow is used, and all the velocity gradients used to compute the L waves are rotated in a direction normal to the flow. After calculating the change in velocities at the boundary, the coordinate system is rotated back. This rotation is accomplished efficiently using a rotation matrix, which allows a generalized three dimensional transformation.

1.4 Object Motion

The motion of the piston and valves needs to be captured accurately in any engine simulation framework. While the two-dimensional valve motion is handled using the mesh blanking method, the one-dimensional piston motion is handled using an accurate energy conserving ALE method.

1.4.1 Mesh Blanking Method

In this approach, the computational mesh is not moved along with the object and the mesh remains fixed corresponding to an Eulerian method. As the object moves, its intersection with the background mesh is calculated and solid-fluid regions are tagged accordingly. The velocity at the boundary cells is updated based on the moving object velocity. No additional modification is required for regions that did not switch from fluid to solid and *vice-versa*. New solid regions that were fluid at the previous instant, can be easily removed from the region that is solved. However, for fluid regions that were solid earlier, no prior time information is available for velocity and other flow quantities. Therefore, this information needs to be reconstructed.

In this work, the quantities of interest are reconstructed using a local gradient minimization method, which accounts for the local boundary conditions. The process is explained here for the velocity of the new fluid cell. For the fluid cell where the velocity needs to be reconstructed, a boundary condition that may be available is the velocity of the object. Another boundary condition is the velocity of the neighboring fluid cells that were not solid in the previous instant. Using this information, a Poisson system of equations is set up for all the new cells created, and this system is solved iteratively to obtain a consistent velocity field. While this method allows for a new layer of fluid cells that is several cells wide, the speed of the object motion is constrained to a few cells to ensure that the computation cost of the Poisson system is small. The error due to neglecting acoustic effects by considering a simple Poisson system is found to be negligible, since this assumption is made in a small volume in the domain. A similar method can be applied for density, pressure and other variables of interest. Different boundary conditions for these variables at the object surface can be imposed depending on the model assumptions.

While the method can be used reasonably for valve motion, the disadvantage of this method is that a large number of solid cells might be present in the simulation if this method is used for objects with a large displacement. For example, if this method is used for the piston

motion, most of the computational cells would be solid at piston top-centre position leading to wasted computational resources. Therefore, a different method is used for handling piston motion.

1.5 Arbitrary Lagrangian Eulerian Method

The Arbitrary Lagrangian Eulerian (ALE) method [16] is a popular method used to solve problems with moving interfaces. The mesh location is moved in a Lagrangian manner, and the effect of this mesh motion is included in the original Eulerian equation as an additional flux. However, the additional fluxes need to be calculated in a consistent manner with other fluxes to preserve overall energy conservation properties. Furthermore, the Discrete Geometric Conservation Law must be satisfied. In this work, the implementation developed in [17] is used which satisfies both of these properties. The method was tested using simple cases such as a box compression and exact mass and energy conservation was obtained.

The time step in the simulation is constrained to prevent mesh overlapping and folding. Since the top of the cylinder does not move, a mesh velocity profile needs to be specified between the object and a stationary location. Some possible choices for this profile are a linear function or an exponential function to minimize the number of cells with large mesh motion. However, both of these functions can lead to poor mesh quality in an actual engine geometry. Instead, the key grid approach [18] is used, where target meshes at different piston locations are generated. The mesh velocity profile is then obtained by computing the relative displacement of different points between the target grids. This allows a controlled and smooth mesh motion with good mesh quality throughout the simulation.

2 VALIDATION

In this section, different validation cases considered to test the simulation framework are presented.

2.1 Flow Bench Simulation

Different flow bench configurations are simulated using the framework presented above. The results are compared against experimental values to assess the quality of the flow solution obtained, which is important for accurate engine LES studies. First, a simple axisymmetric valve setup with detailed mean and fluctuating velocity experimental data is simulated. Next, results from the simulation of an experimental flow bench setup with the full engine geometry are compared against experiments.

2.2 Axisymmetric Flow Bench

The simplified axisymmetric flow bench setup considered here, has been studied previously to assess the quality of the flow solution [19]. It has also been studied using the LES framework [20]. A structured grid is first developed to represent the axisymmetric valve geometry that is shown in Figure 3. The mesh is stretched in order to better resolve regions of interest. The total mesh size is 6.6 million points. A turbulent pipe computed in a separate simulation, is introduced upstream of the valve in the annulus with a mean velocity of 65 m/s. The valve lift for this case is 10 mm and the cylinder diameter is 60 mm. More details on the geometry are available in [19]. The instantaneous velocity field is shown in Figure 3 for a plane through the center of the valve. For the following discussion, the axial direction is z with positive z pointing downwards; the radial direction is r; and the azimuthal direction is x. The W and U velocities are the axial and azimuthal velocities, respectively. The value of z at the valve is zero. The results are compared with experiments at two different locations in the plane of the cylinder. The two locations are 0.02 m and 0.07 m downstream of the bulkhead and are designated as A and B in Figure 3, respectively. The statistics are

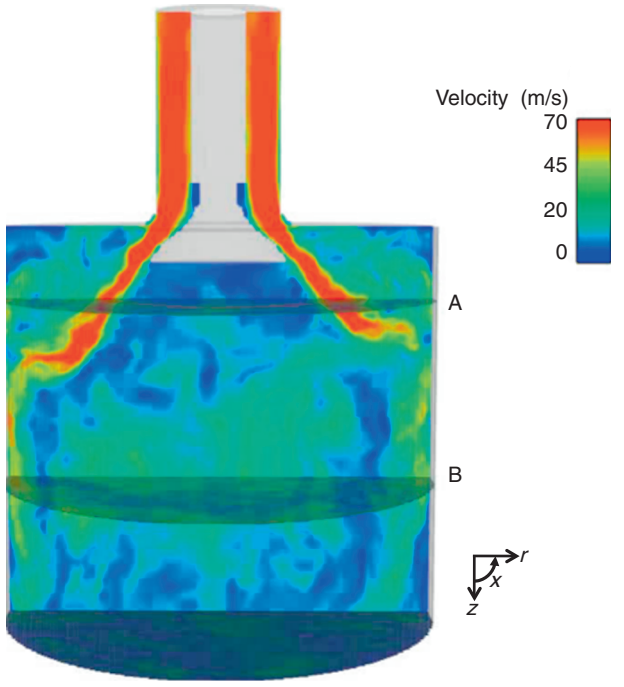

Figure 3

Velocity field from the simulation of the axisymmetric valve configuration.

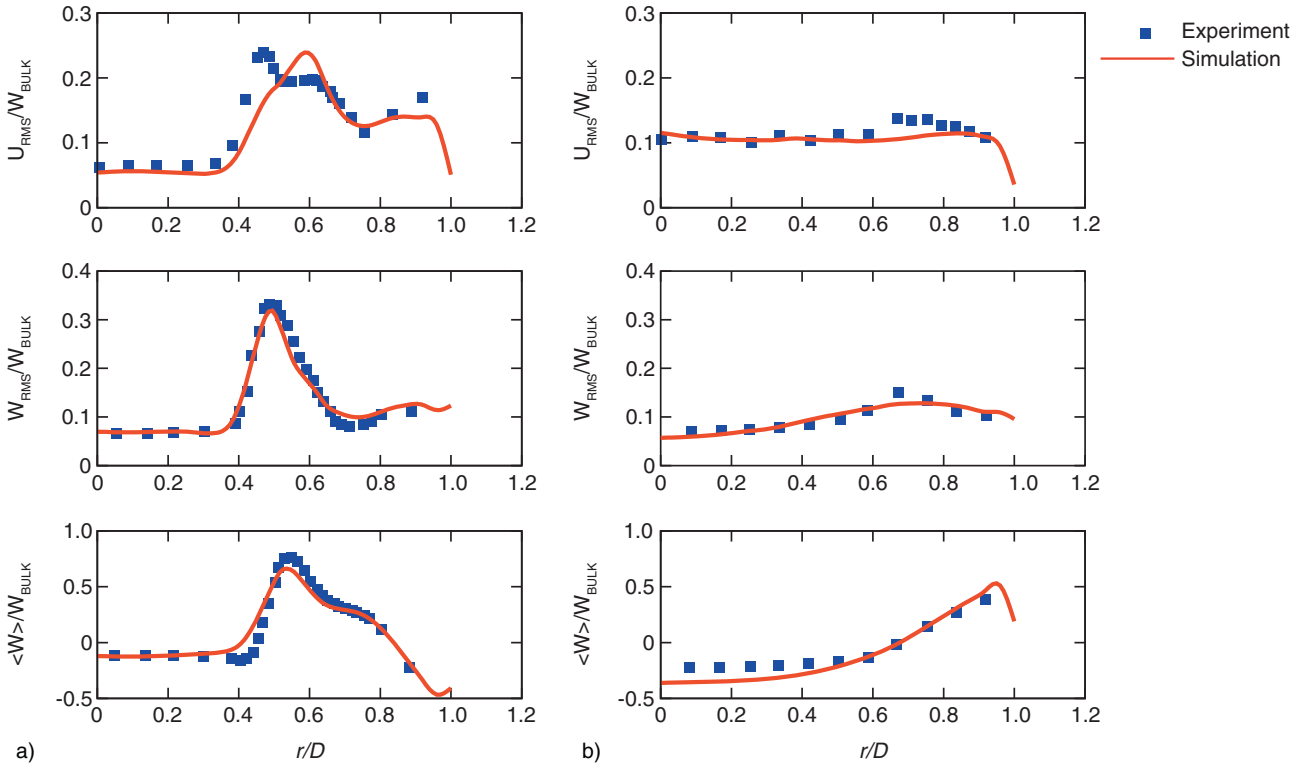

Figure 4

Comparison of the axisymmetric flowbench against experiments. a) The results in the left column are at location, b) and the results in the right column are at location.

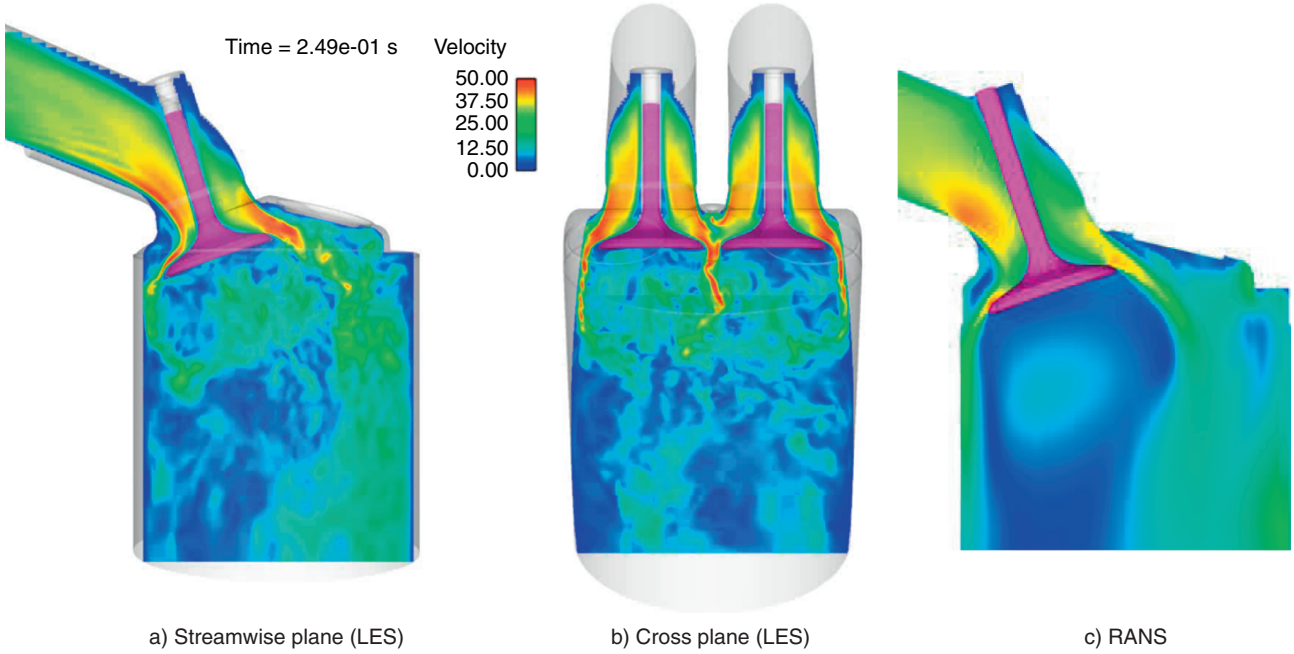

Figure 5

Velocity field obtained using LES and RANS of the engine flow bench configuration. a,b) The instantaneous LES field is shown, c) while the averaged RANS field is shown.

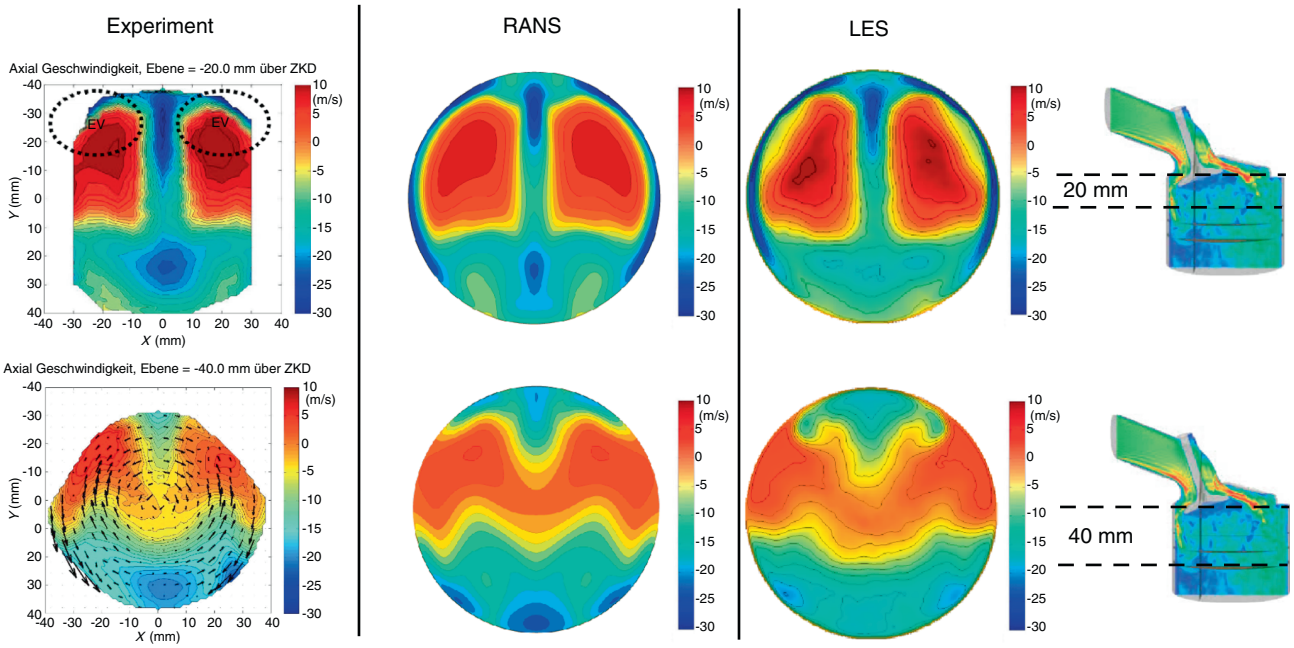

Figure 6

Comparison of the simulated and experimental results for the axisymmetric flowbench.

averaged temporally and also spatially in the azimuthal direction since the configuration is axisymmetric. The radial profile of the mean and fluctuations of the axial velocity and the azimuthal velocity fluctuation are compared with experiments at both locations. The comparison of the simulation results to the experimental data is shown in Figure 4. All results have been scaled by the mean axial velocity W_{BULK}, equal to 65 m/s. Good agreement is obtained for both the mean and the fluctuating velocity statistics at both locations considered. Therefore, the simulation adequately predicts the flow in this configuration.

2.3 Engine Flow Bench

Next, a simulation of the flow bench of an actual engine geometry shown in Figure 5 is performed. The stationary valve lift studied for this configuration is 9.15 mm. The cylinder diameter is 82 mm, and the length is 60 mm. Two intake manifolds with a length of 50 mm are considered in the simulation setup. The diameter of the intake manifolds is 30 mm. Air is the medium used in this flow bench configuration. The mean velocity through the intake manifold is 27.98 m/s corresponding to a mass flow rate of 0.038 kg/s into the cylinder. The Reynolds number associated with these conditions is 47 000, which is in the turbulent flow regime. Therefore, a separate simulation of a fully developed turbulent pipe flow is performed. The velocity profile from this simulation is imposed at the intake manifold of the engine at specified time intervals. The pipe is rotated such that the velocity plane orients exactly with the intake plane in the flow bench simulation. The complex engine geometry is represented in this work using a three-dimensional Cartesian structured grid. Different grids of sizes up to 22 million are used for this study. The simulation is run on 256 processors for 15 days to obtain statistically converged solutions. The results from a RANS simulation of this configuration are also included for comparison. The RANS simulation is performed at Robert Bosch Research and Technology Center using the Fluent commercial software.

An instantaneous snapshot of the velocity field from the LES simulation is shown in Figure 5 at two different planes along with the average velocity field. The corresponding image for the RANS simulations is shown in the right plot in Figure 5. The first plane is aligned with the streamwise direction of the intake manifold, while the other plane in a cut plane through the two valve centers. While the instantaneous LES velocity field has more turbulent structures than the RANS simulation result, the mean results of the LES are quantitatively similar to the results of the RANS simulation for this statistically stationary configuration. Contour plots showing

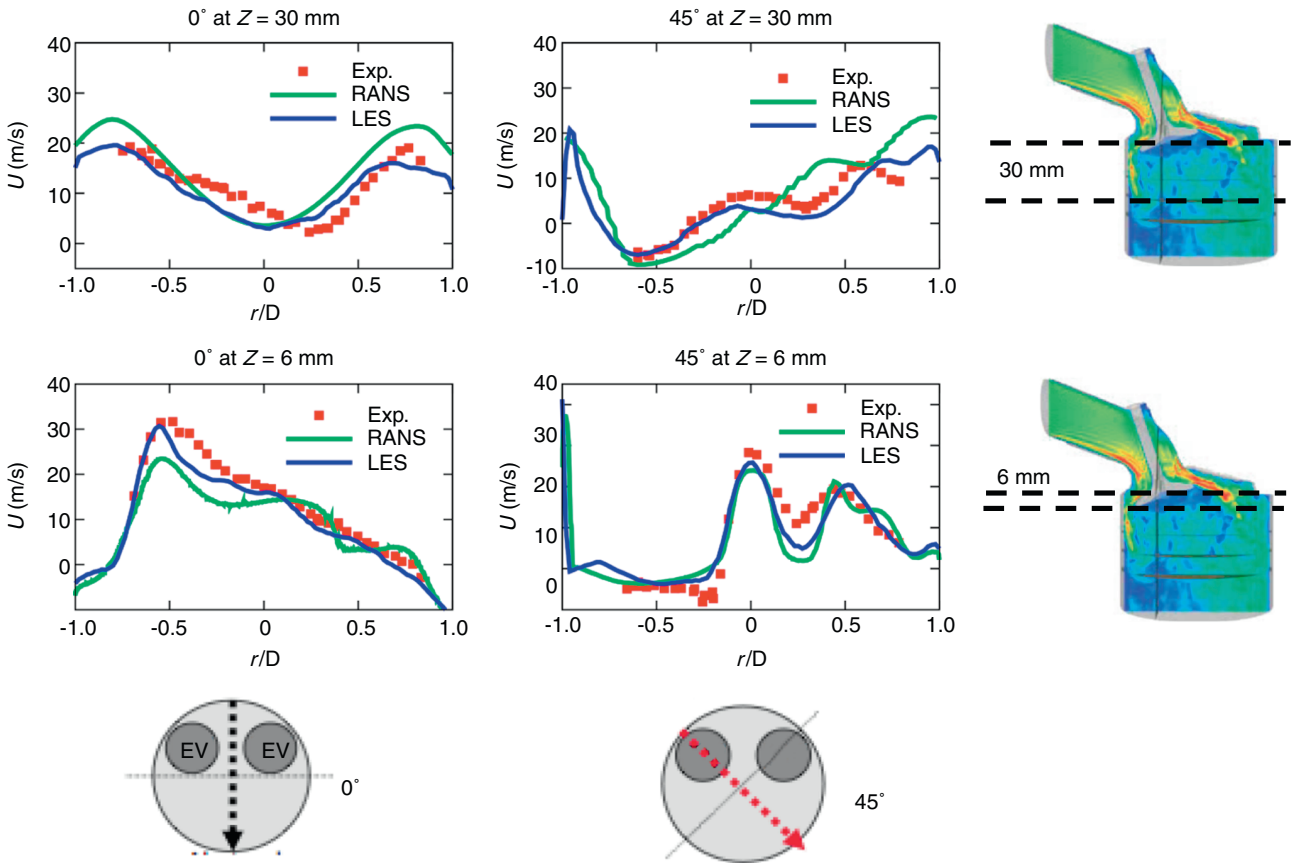

Figure 7

Comparison of the average velocity field in the engine flow bench against experiments.

the comparison of the axial velocity at different locations downstream of the valve are shown in Figure 6. The LES results are averaged over several flow through times. As shown, both the LES and RANS results have the same qualitative structures as compared to the experiments. Next, quantitative comparisons at locations 6 mm and 30 mm below the valve are shown in Figure 7. For both locations, LES results are in better agreement with the experimental results than the RANS results. While this difference is small in this steady state configuration, a bigger difference might be observed when actual engine operation is simulated. Overall, the framework can accurately predict the turbulent flow in a real engine configuration.

3 GAS EXCHANGE SIMULATION

A simulation of a gas exchange in an engine is performed next to assess the accuracy of the simulation in the presence of object motion. The engine is motored at a speed of 2 000 rpm for the configuration studied. The engine cylinder head geometry is the same as that of the flow bench and the compression ratio of the setup is 13. The normalized lift profiles of the intake valve and the exhaust valve are shown in Figure 8. The maximum intake valve lift is 4.06 mm, and the maximum exhaust valve lift is 4.01 mm. The piston displacement profile is also included in this figure. Positive piston displacement denotes downward motion of the piston, and zero displacement is at the location of maximum compression (top center). The maximum piston displacement is 85 mm, and the lowest location is termed as bottom center. The timescale is represented as Crank Angle Degrees (CAD), which represents angular displacement of the crankshaft connected to the piston. At an engine speed of 2 000 rpm, one CAD corresponds to 83.3 μs.

The simulation infrastructure for flow bench simulations is used here. The full engine geometry is discretized using a grid of size 31.5 million grid points. Good

parallel scaling of the code is obtained for 1 024 processors. The motion of the piston, intake valve, and exhaust valve is prescribed using the profiles shown earlier in Figure 8. Object motion is included using the mesh blanking method for valves, and the ALE method for the piston. If a single mesh is compressed using the ALE method over the entire piston displacement, the grid spacing at maximum compression is very small. The maximum allowable timestep in the simulation is directly proportional to this grid spacing to ensure stability. Therefore, a smaller grid spacing leads to smaller timesteps and consequently, a substantial increase in the total simulation runtime. This is avoided by using four different key grids to resolve different piston displacements. The transition points between the different grids are at 15 mm, 27 mm and 37 mm. At each grid transition location, the solution is interpolated between meshes.

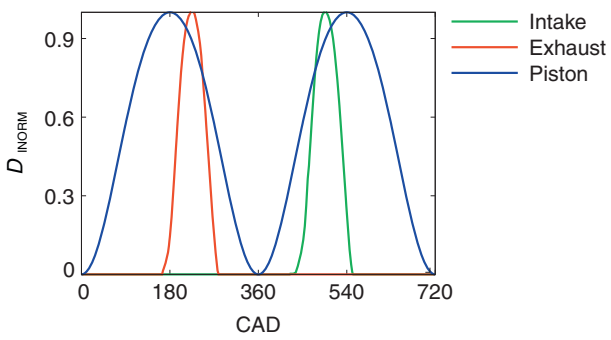

Figure 8

Displacement profiles of the piston, intake valve, and exhaust valve in the gas exchange simulation. All the displacements have been divided by the maximum displacement to obtain a normalized displacement, D_{NORM}.

The boundary condition at the intake and exhaust manifolds is prescribed using the NSCBC procedure described earlier. The target pressure at the intake and exhaust manifolds is obtained experimentally. The representative length scale L_i, in Equation (4) is set as 5 mm for the simulation. The choice of this value, which is small compared to the intake manifold length of 50 mm, ensures that the pressure in the simulation relaxes quickly to the experimental pressure at the boundary. An additional non-reactive scalar is also tracked to visualize mixing in the cylinder. It is initially prescribed as one in the cylinder and exhaust manifold

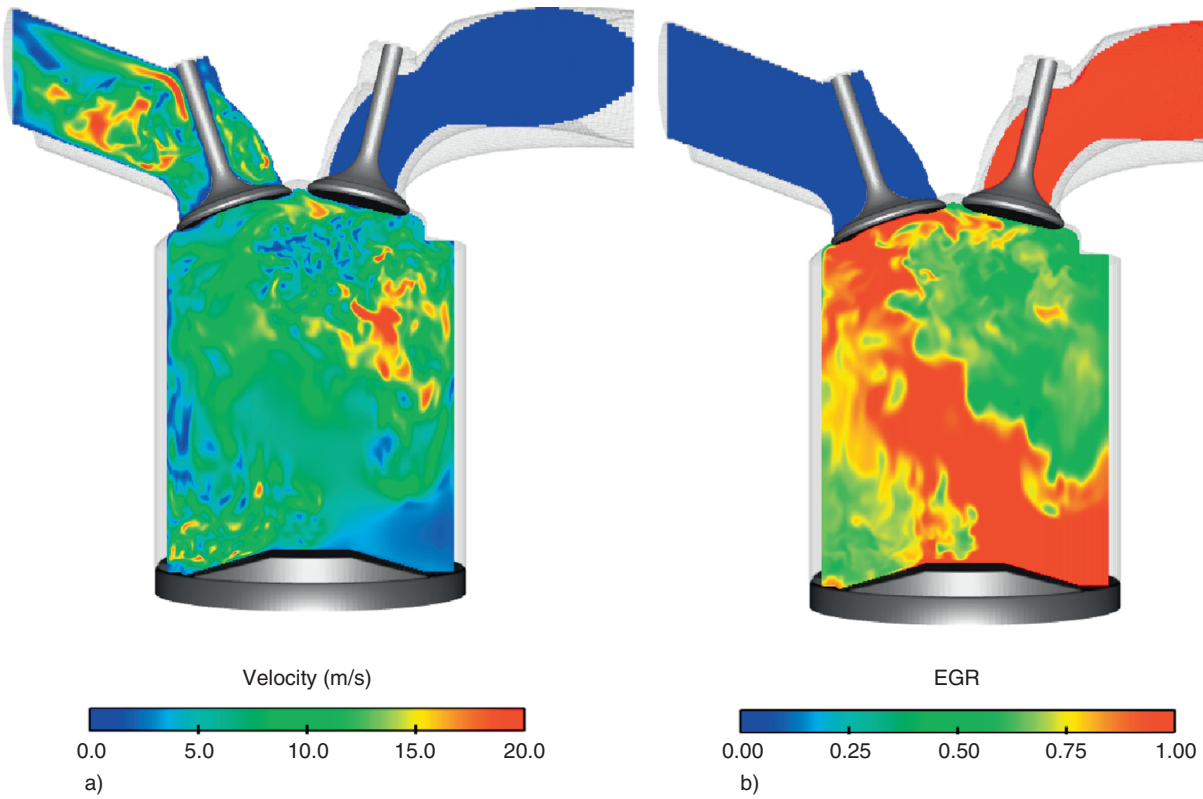

Figure 9

Two-dimensional plane depicting a) the velocity field and b) mixing field from the gas exchange simulation at 565 CAD.

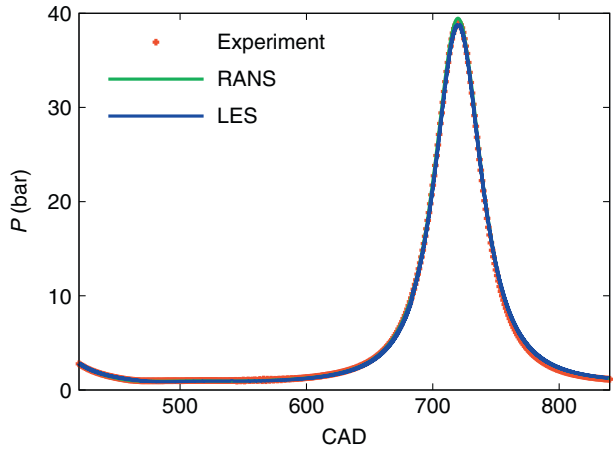

Figure 10

Average pressure in the cylinder compared against experiments.

and zero in the intake manifold. This scalar is a representation of residual exhaust gases (EGR) in the cylinder.

A two-dimensional plane of the velocity and mixing field after closing of the intake valve is shown in Figure 9. Both the fields depict the turbulent mixing and the different flow scales in the cylinder. Overall, at all time instants, the fields obtained using the simulation seem physically reasonable. While velocity fields cannot be compared to experiments due to a lack of data, the pressure in the cylinder is compared between LES and experiments in Figure 10. Results from a RANS calculation are also compared. Overall, good agreement is obtained over the entire cycle as compared to RANS and experiment. However, the peak pressure is not exactly predicted by the LES calculation. Based on further analysis, this discrepancy is caused by differences in the mass flow when the intake valve is first opened. In the LES study, the timing when the valve opens enough for significant mass flow, is later than the RANS study. This discrepancy occurs due to inadequate resolution near the valves, leading to an artificial closure of flow passages between the valve and the engine. This effect is exaggerated here because for this specific engine, the valve is held open initially at a small lift for a considerable time. Due to this discrepancy, the total mass in the cylinder is underpredicted in the LES study, leading to a small discrepancy in the maximum pressure. Another simulation using a refined grid with 48 million points is performed to analyze this effect. It is found that the mass profile is the same for this grid as the other LES grid. Therefore, considerably more resolution is required to accurately capture this effect.

However, other than this discrepancy, the LES simulation provides accurate results for this configuration, and can be used for performing LES of internal combustion engines after resolving this issue. In the future, methods such as local grid refinement [21] or overset grid methods [22], will be integrated with this framework to provide additional resolution near the valves without adding significant computational cost.

CONCLUSION

A structured framework for LES of IC engines is presented in this work. The framework is based on discretely energy conserving schemes for accurate LES simulations. Methods are presented for handling motion of the piston and valves. Modification to the widely used NSCBC method is presented to allow for realistic manifold boundary conditions. Various canonical test cases are studied to evaluate the performance of this framework. Good comparison is obtained for flow in a simplified axisymmetric configuration and a real engine. The flow in a motored engine is also reasonably predicted overall. However, additional methods such as overset meshes need to be used near valves to adequately resolve the flow in those regions.

ACKNOWLEDGMENTS

The material is based upon work supported by the Department of Energy [National Energy Technology Laboratory] under Award number DE-EE0003533. The work is performed as a part of the ACCESS project consortium (Robert Bosch LLC, AVL Inc., Emitec Inc.) under the direction of PI Hakan Yilmaz, Robert Bosch LLC.

REFERENCES

1 Rutland C.J. (2011) Large-eddy simulations for Internal combustion engines - a review, *Int. J. Eng. Res.* 421-451.

2 Enaux B., Granet V., Vermorel O., Lacour C., Pera C., Angelberger C., Poinsot T. (2011) LES study of cycle-to-cycle variations in a spark ignition engine, *Proc. Combust. Inst.* **33**, 2, 3115-3122. ISSN 1540-7489.

3 Goryntsev D., Sadiki A., Klein M., Janicka J. (2010) Analysis of cyclic variations of liquid fuel-air mixing processes in a realistic DISI IC-engine using Large Eddy Simulation, *Int. J. Heat Fluid Flow* **31**, 5, 845-849. ISSN 0142-727X.

4 Hasse C., Sohm V., Durst B. (2010) Numerical investigation of cyclic variations in gasoline engines using a hybrid URANS/LES modeling approach, *Comput. Fluids* **39**, 1, 25-48. ISSN 0045-7930.

5 Vermorel O., Richard S., Colin O., Angelberger C., Benkenida A., Veynante D. (2009) Towards the understanding of cyclic variability in a spark ignited engine using multi-cycle LES, *Combust. Flame* **156**, 8, 1525-1541, ISSN 0010-2180.

6 Vasilyev O.V. (2000) High order finite difference schemes on non-uniform meshes with good conservation properties, *J. Comput. Phys.* **157**, 2, 746-761.

7 Germano M., Piomelli U., Moin P., Cabot W.H. (1991) A dynamic subgrid-scale eddy viscosity model, *Phys. Fluids A: Fluid Dyn.* **3**, 7, 1760-1765.

8 Meneveau C., Lund T.S., Cabot W.H. (1996) A Lagrangian dynamic subgrid-scale model of turbulence, *J. Fluid Mech.* **319**, 353-385.

9 Balarac G., Pitsch H., Raman V. (2008) Development of a dynamic model for the subfilter scalar variance using the concept of optimal estimators, *Phys. Fluids* **20**, 3, 035114.

10 Desjardins O., Blanquart G., Balarac G., Pitsch H. (2008) High order conservative finite difference scheme for variable density low Mach number turbulent flows, *J. Comput. Phys.* **227**, 7125-7159.

11 Stanescu D., Habashi W.G. (1998) 2n-storage low dissipation and dispersion Runge-Kutta schemes for computational acoustics, *J. Comput. Phy.* **143**, 2, 674-681.

12 Gaitonde V.D., Visbal M.R. (1998) High-order schemes for Navier-Stokes equations: Algorithm and implementation into FLD3DI. (AFRL-VA-WP-TR-1998-3060), 21.

13 Mittal R., Iaccarino G. (2005) Immersed boundary methods, *Annu. Rev. Fluid Mech.* **37**, 1, 239-261.

14 Poinsot T.J., Lele S.K. (1992) Boundary conditions for direct simulations of compressible viscous flows, *J. Comput. Phys.* **101**, 104-129.

15 Lodato G., Domingo P., Vervisch L. (2008) Three-dimensional boundary conditions for direct and large-eddy simulation of compressible viscous flows, *J. Comput. Phys.* **227**, 5105-5143.

16 Hirt C.W., Amsden A.A., Cook J.L. (1974) An arbitrary Lagrangian-Eulerian computing method for all flow speeds, *J. Comput. Phys.* **14**, 3, 227-253.

17 Shashank, Pitsch H. (2008) Large eddy simulation of internal combustion engine processes with immersed boundary technique, *International Conference LES for Internal Combustion Engine Flows*, 1-2 Dec. Rueil-Malmaison, France.

18 Duclos J.M., Zolver M. (1998) 3D modeling of intake, injection and combustion in a DI-SI engine under homogeneous and stratified operating conditions, *Proceedings of the Fourth International Symposium COMODIA* **98**, 335-340.

19 Thobois L., Rymer G., Souleres T., Poinsot T. (2004) Large-eddy simulation in IC engine geometries, *SAE Technical Paper* 2004-01-1854.

20 Shashank S., Kang S., Pitsch H. (2009) Application of immersed boundary technique for large eddy simulation of IC engine processes, *Academy colloquium on immersed boundary methods: current status and future research directions*, 15-17 June, Amsterdam, The Netherlands.

21 Ferziger J.H., Peric M. (2001) *Computational Methods for Fluid Dynamics*, Springer-Verlag.

22 Meakin R.L. (2000) Adaptive spatial partitioning and refinement for overset structured grids, *Comput. Meth. App. Mech. Eng.* **189**, 4, 1077-1117.

Manuscript accepted in December 2012
Published online in October 2013